EARTHQUAKE ENGINEERING AND STRUCTURAL DYNAMICS
Earthquake Engng Struct. Dyn. 2007; **36**:1741–1761
Published online 13 July 2007 in Wiley InterScience (www.interscience.wiley.com). DOI: 10.1002/eqe.716

Seismic demands on secondary systems in base-isolated nuclear power plants

Yin-Nan Huang[1,*,†], Andrew S. Whittaker[1], Michael C. Constantinou[1] and Sanjeev Malushte[2]

[1]*State University of New York at Buffalo, New York, NY 14260, U.S.A.*
[2]*Bechtel Power Corporation, Frederick, MD 21703, U.S.A.*

SUMMARY

Numerical models of a sample nuclear power plant (NPP) reactor building, both conventionally constructed and equipped with seismic protective systems, are analysed for both safe shutdown and beyond-design-basis earthquake shaking at two coastal sites in the United States. Seismic demands on secondary systems are established for the conventional and seismically isolated NPPs. The reductions in secondary-system acceleration and deformation demands afforded by the isolation systems are identified. Performance spaces are introduced as an alternate method for evaluating demands on secondary systems. The results show that isolation systems greatly reduce both the median and dispersion of seismic demands on secondary systems in NPPs. Copyright © 2007 John Wiley & Sons, Ltd.

Received 5 October 2005; Revised 15 April 2007; Accepted 17 April 2007

KEY WORDS: nuclear power plant; secondary systems; seismic base isolation; viscous dampers; performance spaces

1. INTRODUCTION

The U.S. Nuclear Regulatory Commission (USNRC) Regulatory Guide RG 1.165 [1] specifies that the safe shutdown earthquake (SSE) for the seismic design of safety-related nuclear structures be based on a 5% damped median response spectrum with a return period of 100 000 years (or a median annual probability of exceedance of 1×10^{-5}). Chapter 1 in title 10 of the Code of Federal Regulations [2] describes that safety-related structures, secondary systems and components must remain functional (undamaged) in the event of SSE shaking. For many nuclear power plant (NPP) and spent nuclear fuel (SNF) sites in the U.S., earthquake shaking associated with the SSE will

*Correspondence to: Yin-Nan Huang, State University of New York at Buffalo, 212 Ketter Hall, Buffalo, NY 14260, U.S.A.
†E-mail: yh28@buffalo.edu

Contract/grant sponsor: National Science Foundation (NSF); contract/grant number: EEC-9701471
Contract/grant sponsor: The State of New York

result in high seismic acceleration and deformation demands in the stiff NPP structural systems and extremely high demands on the safety-related secondary systems.

Seismic protective systems, herein assumed to include seismic isolation and damping devices, can substantially mitigate these high demands on primary structural components and secondary mechanical, electrical and piping systems, by reducing the natural frequency of the NPP structure and thus enable direct reductions in overnight capital cost and standardization of NPP and SNF facility designs and simplified design and regulatory review; facilitate design certification and the granting of early site permits and construction and operating licenses; and enhance NPP and SNF safety at lower capital cost.

Seismic isolation and damping systems are widely used to protect mission-critical infrastructure. More than 3000 buildings, bridges, and other types of structures have been base isolated to date [3] but there are only six applications to NPPs: four in France and two in South Africa [4]. Guidelines for the seismic isolation of NPPs have been prepared in Japan and the United States [5, 6]. Much of the research work on the protection of secondary systems using seismic isolation was published in the 1980s, with an emphasis on horizontal isolation systems. Buckle *et al.* [4] reviewed several feasibility studies related to the application of isolation systems to NPPs performed in the early 1980s. Fan and Ahmadi presented numerical results for the seismic response of secondary systems in a three-storey base-isolated structure [7]. Kelly and Tsai performed a series of earthquake simulator tests with a five-storey steel frame to identify the influence of rubber-bearing isolation systems on seismic response of light secondary equipments [8, 9]. Khechfe *et al.* proposed an experimental study of a base-isolated secondary system installed on a fixed-base three-storey frame [10]. All the numerical and physical simulation studies showed significant reductions in the seismic response of secondary systems through the use of properly designed isolation systems. Studies on vertical isolation systems are few in number. A five-year research project on three-dimensional (3-D) isolation systems has been completed [11–14] in which the investigators proposed complex devices to reduce the *rocking* response of the isolated containment vessel.

The primary focus of this paper is the characterization of seismic demands on secondary systems in conventional and seismic-protected NPP construction because the costs associated with analysis, design, construction, testing, and regulatory approval of secondary systems can dominate the cost of NPPs. Substantial reductions in demands on secondary systems such as steam generators and piping systems will facilitate greater use of commercial-off-the-shelf equipment, simplify system and equipment qualification and design and regulatory review, and enhance NPP safety.

Interaction between the primary structure and secondary systems is not addressed herein because the mass ratios for secondary systems are typically very low: less than 3% for the heaviest secondary system in the sample reactor building considered here. Moreover, the interaction is insignificant for the isolated reactor building because the frequency ratio of the primary structure and secondary systems is more than 10. Others have shown that significant primary structure–secondary system interaction occurs as the mass ratio of the secondary and primary systems increases and the frequency ratio approaches 1.0 [15–17]. The interaction between the primary and secondary systems for an isolated building may be of concern if the secondary system is heavy and tuned to a higher mode frequency in the primary system.

The potential benefits of applying seismic protective systems to the next generation of NPPs and SNF buildings prompted the study described in the remainder of this paper. Response-history analysis of numerical models of conventional and base-isolated (termed isolated hereafter) NPP reactor buildings was used to assess demands on structural and secondary systems. Herein, attention is focused on isolation for horizontal earthquake shaking only.

DOI: 10.1002/eqe

2. RESPONSE-HISTORY ANALYSIS

2.1. Dynamic models of the fixed-base and base-isolated reactor buildings

Figure 1(a) shows a cutaway view of a NPP reactor building of conventional construction. A lumped-mass stick model of this reactor building was used to benchmark results from response-history analysis. (Information on the framing of the NPP reactor building was provided by a NPP supplier.) The model, shown in Figure 1(b) and (c), is composed of two *sticks*: one representing

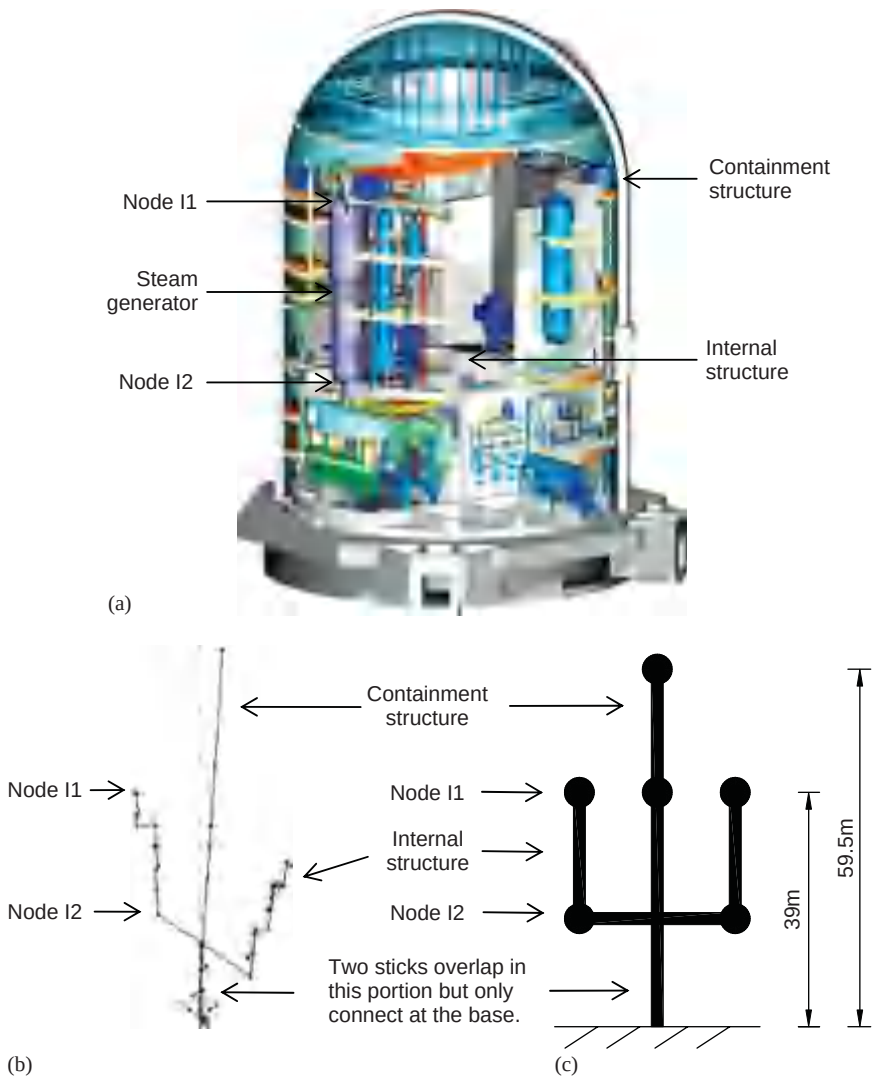

Figure 1. Sample NPP reactor building and stick model for response-history analysis: (a) cutaway view of NPP reactor building; (b) model 1 and first mode shape in SAP2000; and (c) stick model.

DOI: 10.1002/eqe

Table I. Description of response-history-analysis models.

Model no.	Type of bearings	Description*
1	None	First mode periods of the containment and internal structures, in each horizontal direction, are (0.22, 0.21 s) and (0.14, 0.13 s), respectively
2	FP isolated	$\mu_{max} = 0.03$; $\mu_{min} = 0.015$; $a = 55\,\text{s/mm}$; $T_d = 3\,\text{s}$; $u_y = 1\,\text{mm}$
3	FP isolated	$\mu_{max} = 0.03$; $\mu_{min} = 0.015$; $a = 55\,\text{s/mm}$; $T_d = 4\,\text{s}$; $u_y = 1\,\text{mm}$
4	FP isolated	$\mu_{max} = 0.06$; $\mu_{min} = 0.03$; $a = 55\,\text{s/mm}$; $T_d = 3\,\text{s}$; $u_y = 1\,\text{mm}$
5	FP isolated	$\mu_{max} = 0.06$; $\mu_{min} = 0.03$; $a = 55\,\text{s/mm}$; $T_d = 4\,\text{s}$; $u_y = 1\,\text{mm}$
6	FP isolated	$\mu_{max} = 0.09$; $\mu_{min} = 0.04$; $a = 55\,\text{s/mm}$; $T_d = 3\,\text{s}$; $u_y = 1\,\text{mm}$
7	FP isolated	$\mu_{max} = 0.09$; $\mu_{min} = 0.04$; $a = 55\,\text{s/mm}$; $T_d = 4\,\text{s}$; $u_y = 1\,\text{mm}$
8	LR isolated	$Q_d = 0.03W$; $T_d = 2\,\text{s}$; $K_u = 10K_d$
9	LR isolated	$Q_d = 0.03W$; $T_d = 3\,\text{s}$; $K_u = 10K_d$
10	LR isolated	$Q_d = 0.06W$; $T_d = 2\,\text{s}$; $K_u = 10K_d$
11	LR isolated	$Q_d = 0.06W$; $T_d = 3\,\text{s}$; $K_u = 10K_d$
12	LDR isolated	$T_d = 2\,\text{s}$; $\beta_i = 0.03$
13	LDR isolated	$T_d = 3\,\text{s}$; $\beta_i = 0.03$
14	HDR isolated	$T_d = 2\,\text{s}$; $\beta_i = 0.10$
15	HDR isolated	$T_d = 3\,\text{s}$; $\beta_i = 0.10$
16	HDR isolated	$T_d = 2\,\text{s}$; $\beta_i = 0.20$
17	HDR isolated	$T_d = 3\,\text{s}$; $\beta_i = 0.20$

*See Figure 2 for definitions of Q_d, K_d, and K_u and Equation (1) and Figure 3 for those of μ_{max}, μ_{min}, and a; T_d is related to K_d through the supported weight; T_i is the isolated period based on a rigid superstructure; β_i is the damping in the HDR isolation systems.

the containment structure and the other representing the internal structure. The two sticks are structurally independent and are connected only at the base. The mechanical properties of the frame elements that compose each stick were back-calculated from analysis of the 3-D reactor building using industry-standard procedures. The reactor building was assumed to be founded on *West Coast* rock. The mass of the structure and the secondary systems was lumped at discrete locations at key levels in the reactor building. Since the mass of the primary and secondary systems was lumped together, interaction between the primary and secondary systems could not be considered. The discrete masses were connected to the frame elements through rigid links to account for torsional effects. The total height of the containment structure is 59.5 m and its first mode period is approximately 0.2 s. The height of the internal structure is 39 m; the first mode period of the internal structure in both horizontal directions is approximately 0.14 s. The total weight of the NPP reactor building is approximately 75 000 tons.

Seventeen numerical models were developed in the computer code SAP2000 Nonlinear [18] to study the impact of seismic protective systems on the response of the NPP reactor building and its secondary systems. Table I lists the properties of the isolation system for each model. Model 1 is for the conventionally framed NPP reactor building. Models 2–17 include representations of Friction Pendulum™ (FP) bearings, lead–rubber (LR) bearings, low damping rubber (LDR) bearings and high damping rubber (HDR) bearings. Bilinear plasticity elements were used for the LR bearings. Figure 2 shows the key variables defining the bilinear hysteresis loop. For FP bearings, the velocity dependence of the coefficient of sliding friction is given by [19–21]

$$\mu = \mu_{max} - (\mu_{max} - \mu_{min}) \cdot e^{-aV} \tag{1}$$

DOI: 10.1002/eqe

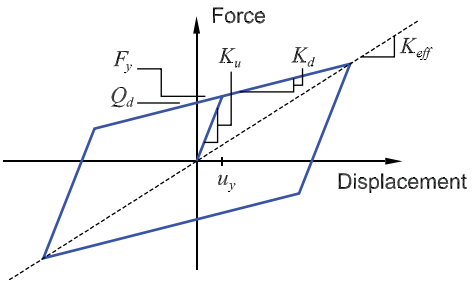

Figure 2. Assumed properties of the LR and Coulomb-friction-FP bearings.

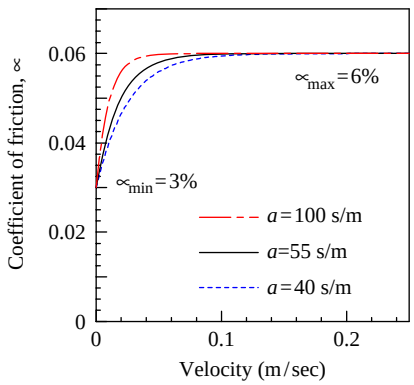

Figure 3. The influence of a on the velocity dependence of the coefficient of sliding friction.

where μ is the coefficient of sliding friction, varying between μ_{max} and μ_{min} (obtained at high and very small velocities, respectively), a is a velocity-related parameter, and V is the sliding velocity. Figure 3 shows the velocity dependence of μ for a typical FP PTFE-type composite material in contact with polished stainless steel for a typical contact (normal) pressure of approximately 41 MPa (6 ksi). For this pressure, $\mu_{max} = 6\%$, $\mu_{min} = 3\%$, and $a = 55$ s/m. A value of $a = 55$ s/m was adopted for the study described herein. The influence of a on the velocity dependence of μ is shown in Figure 3 for $a = 40$, 55, and 100 s/m.[‡]

To study a wide range of isolator properties,[§] Q_d of Figure 2 was set equal to either 3 or 6% of the supported weight W for the LR bearings and μ_{max} was set equal to 3, 6, or 9% for the FP bearings, where for Coulomb friction, $Q_d = \mu_{max} W$. The second-slope period (related to K_d of Figure 2 through the supported weight) was assigned values of 2 and 3 s for the LR bearings, and 3 and 4 s for the FP bearings. The LDR and HDR bearings were modelled as linear viscoelastic elements. The linear viscoelastic models could also model an isolation system incorporating LDR bearings and linear viscous dampers. Again, to study a wide range of isolator properties, consistent

[‡]The hysteresis loop for the FP bearing will converge to the bilinear loop shown in the Figure 2 for Coulomb friction ($a = \infty$).

[§]The mechanical properties (periods) of the isolators were limited to those of practical significance.

DOI: 10.1002/eqe

with isolators used in design practice, the dynamic properties of the LDR isolators included isolated periods of 2 and 3 s and viscous damping ratios of 3% of critical, and those of the HDR isolators included isolated periods of 2 and 3 s and viscous damping ratios of 10 and 20% of critical, noting that a damping ratio of 20% can only be realized in a HDR isolation system with supplemental damping devices.

2.2. Earthquake histories used for the response-history analysis

To judge the utility of seismic isolation for NPP and SNF applications, response-history analysis was performed using earthquake histories generated for East and West Coast sites. The two bins of 10 pairs of earthquake histories used for the analysis were generated by Somerville *et al.* [22] for firm soil sites in Boston and Los Angeles and a 2% probability of exceedance in 50 years. The Somerville seed motions were re-scaled for the response-history analysis reported herein. Each pair of earthquake histories was scaled to minimize the sum of the squared error between the target spectral values (developed from the USGS hazard maps for a 2% probability of exceedance in 50 years) and the geometric mean of the spectral ordinates for the pair at periods of 0.3, 2, and 4 s, where 0.3 s is the representative of the natural period of a conventionally framed NPP and 2 and 4 s represent two of the isolated periods considered in the study. Acceleration spectra for the resulting 20 histories in each bin are shown in Figure 4(a) and (c) for the East and West Coast sites, respectively. The variability in the spectral ordinates by bin and period is indicative of the scatter in recorded ground motions. Figure 4(b) and (d) present the target spectrum, and

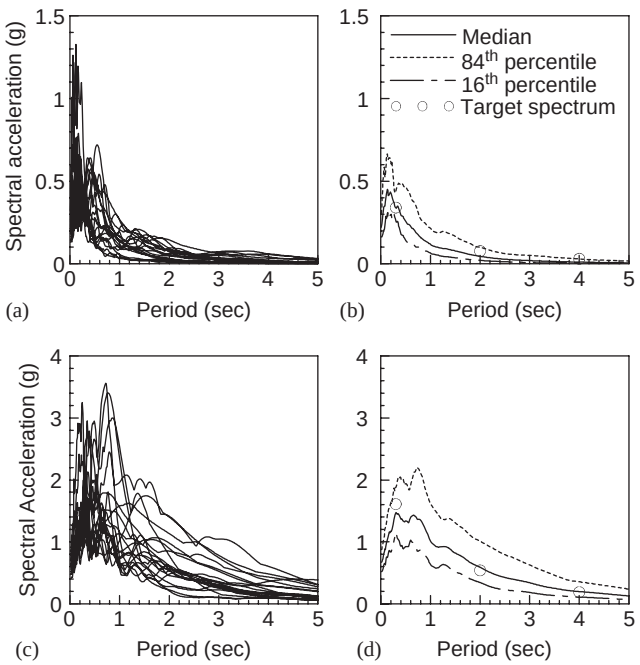

Figure 4. Spectral accelerations of the ground motion bins for Boston and Los Angeles. Boston: (a) all histories and (b) statistics. Los Angeles: (c) all histories and (d) statistics.

DOI: 10.1002/eqe

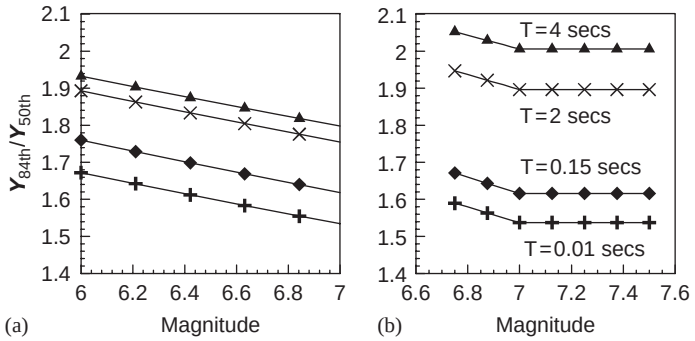

Figure 5. Beyond-design-basis acceleration time-series magnification factors: (a) Campbell [23] for Boston bin and (b) Abrahamson and Silva [24] for Los Angeles bin.

the median, 84th percentile and 16th percentile spectral ordinates for the 20 histories for the East and West Coast sites, respectively. It should be noted that the spectral ordinates of the West Coast (Los Angeles) histories are substantially larger in the long-period range than those of the East Coast (Boston) histories.

The 2% probability of exceedance in 50 years corresponds to the return period of 2475 years: a return period much less than that required by RG 1.165 for SSE shaking. Although this could be considered a shortcoming of the analysis reported herein, the authors felt that it was more important to utilize a robust set of earthquake histories that accounted directly for randomness in the ground motion than to use motions matched to a site-specific spectrum. Importantly, the target spectra of Figure 4(b) and (d) could represent SSE shaking at sites on the East and West Coast, although not in Boston or Los Angeles, respectively.

Safety assessment of a NPP often requires a margin assessment, or an estimate of response for beyond-design-basis (BDB) earthquake shaking, to ensure that shaking in excess of that associated with the SSE spectrum will not substantially compromise the safety and integrity of the NPP structure and its secondary systems. No specific margin or multiplier is mandated by the USNRC for BDB assessment. Per RG 1.165, SSE shaking is characterized by a 5% damped *median* spectrum. For this study, earthquake histories for the BDB assessment were generated by amplifying the acceleration time series for each history from the *median* level to an 84th percentile level. Assume the spectral acceleration, S, at a period is lognormally distributed, so

$$\frac{S_{84\text{th}}}{S_{50\text{th}}} = \frac{\exp(m_{\ln S} + \beta_{\ln S})}{\exp(m_{\ln S})} = \exp(\beta_{\ln S}) \tag{2}$$

where $S_{84\text{th}}$ and $S_{50\text{th}}$ are the 84th percentile and 50th percentile values of S, respectively, and $m_{\ln S}$ and $\beta_{\ln S}$ are mean and standard deviation of $\ln S$. Equation (2) shows that the acceleration time-series magnification factor defined here is related only to $\beta_{\ln S}$. The factor was determined using ground-motion–attenuation relationships for East and West Coast sites. The attenuation relationships of Campbell [23] and Abrahamson and Silva [24] were used to compute the multipliers for the East Coast and West Coast sites, respectively. Values for the multiplier were computed for periods of 0.01, 0.15, 2.0, and 4.0 s. Results are shown in Figure 5. For the BDB assessment presented here, a magnification factor of 1.7 was used to amplitude scale the SSE acceleration histories.

DOI: 10.1002/eqe

Table II. Combinations of earthquake shaking and superstructure strength.

Case	Ground motion	Yield strength of superstructure
I	SSE shaking	∞
II	BDB shaking	V_y
III	BDB shaking	$1.20V_y$
IV	BDB shaking	$1.67V_y$
V	BDB shaking	∞

2.3. Combinations of earthquake shaking and superstructure strength

Response-history analysis was performed for each model and for five combinations of ground shaking and superstructure strength. Table II presents the combinations. Two levels of ground shaking were considered: SSE shaking and BDB shaking, where BDB shaking was 170% of SSE shaking. Four levels of internal superstructure (exclusive of the isolators) strength were considered: infinite (elastic response), V_y, $1.20V_y$, and $1.67V_y$, where V_y in each frame element in each horizontal direction was taken as the median shear force demand of the 20 earthquake histories for SSE shaking on the conventionally framed NPP. Bilinear shear hinges with 10% post-yield stiffness were assigned to all frame elements in the *internal-structure* stick. The containment structure was assumed to remain elastic for SSE and BDB shaking because containment structures are designed for large internal pressures (up to 500 kPa) resulting from a postulated accident, and seismic loadings generally do not control their design. The strengths of $1.20V_y$ and $1.67V_y$ are two estimates of the strength of the internal structural components, considering two strength reduction factors used for the design of reinforced concrete structures: 0.85 ($\simeq 1/1.20$) and 0.6 ($\simeq 1/1.67$). The five superstructure strengths of Table II were assigned to each of the 17 models.

3. SEISMIC DEMANDS ON SECONDARY SYSTEMS

3.1. Response-history analysis results

In this study, unidirectional horizontal earthquake histories were applied to each model along each horizontal axis for a total of 40 simulations per model per bin. The statistical analysis in this section utilizes peak response data from each of the 40 simulations. Results of the response-history analysis are presented below for the internal structure only because the secondary systems are supported primarily on this structure and not the containment vessel. Plotted results are presented in this section for Models 1–15 only because the response data for Models 16 and 17 are similar in magnitude to those of Models 14 and 15, respectively.

Figures 6 and 7 present the maximum acceleration statistics at node I1, the top of the internal structure (as shown in Figure 1), and the drift ratio (relative displacement divided by height) statistics between nodes I1 and I2 for all models, five cases and two bins of earthquake shaking. Accelerations at node I1 characterize peak demands at piping-system attachment points at the top of the internal structure. Nodes I1 and I2 drift ratios represent peak demands on deformation-sensitive components such as steam generators. Median, 16th percentile and 84th percentile values are presented assuming that maximum values obtained from the response-history analysis are lognormally distributed. Table III lists the median response ratios of Figures 6 and 7, calculated as

DOI: 10.1002/eqe

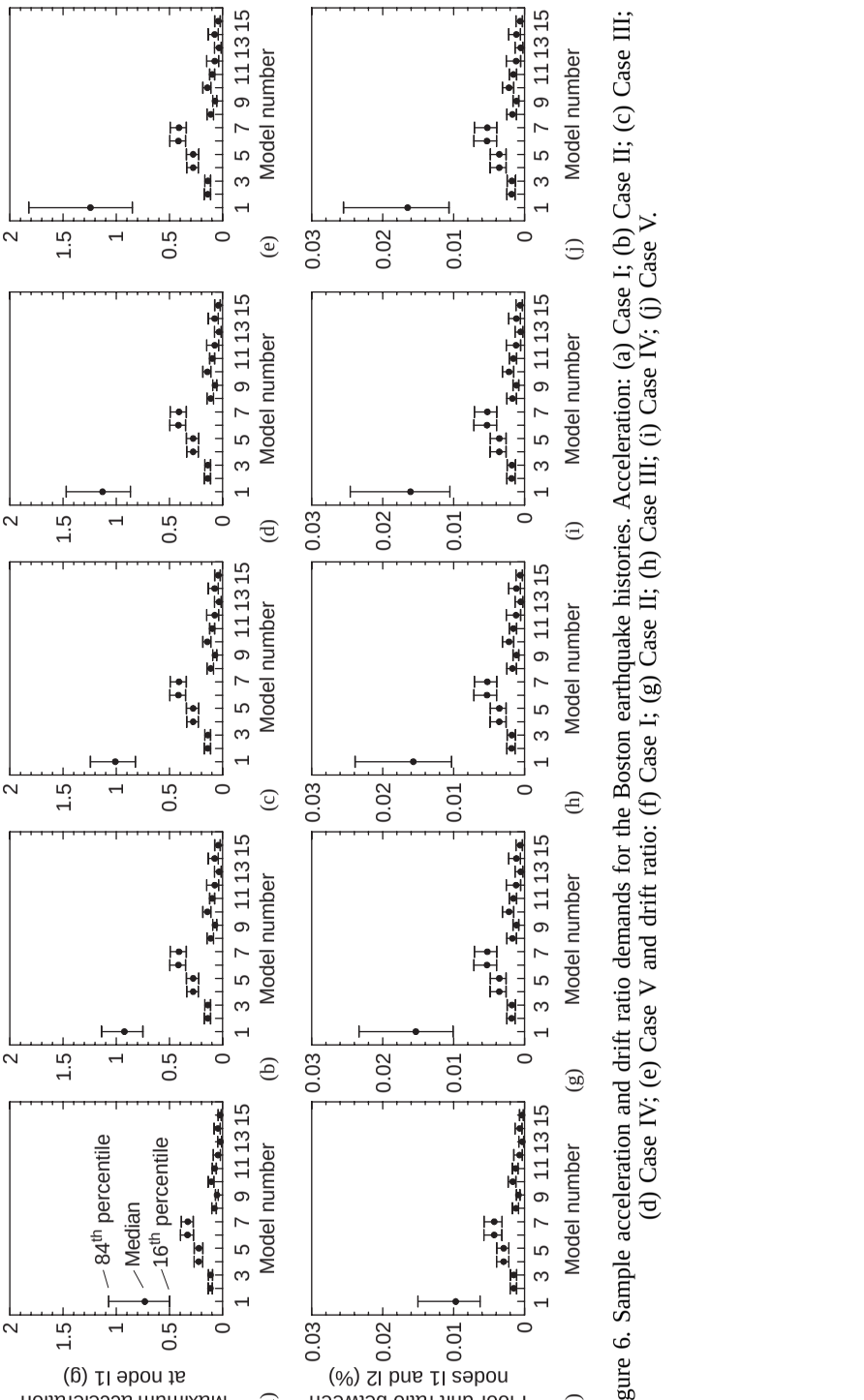

Figure 6. Sample acceleration and drift ratio demands for the Boston earthquake histories. Acceleration: (a) Case I; (b) Case II; (c) Case III; (d) Case IV; (e) Case V and drift ratio: (f) Case I; (g) Case II; (h) Case III; (i) Case IV; (j) Case V.

DOI: 10.1002/eqe

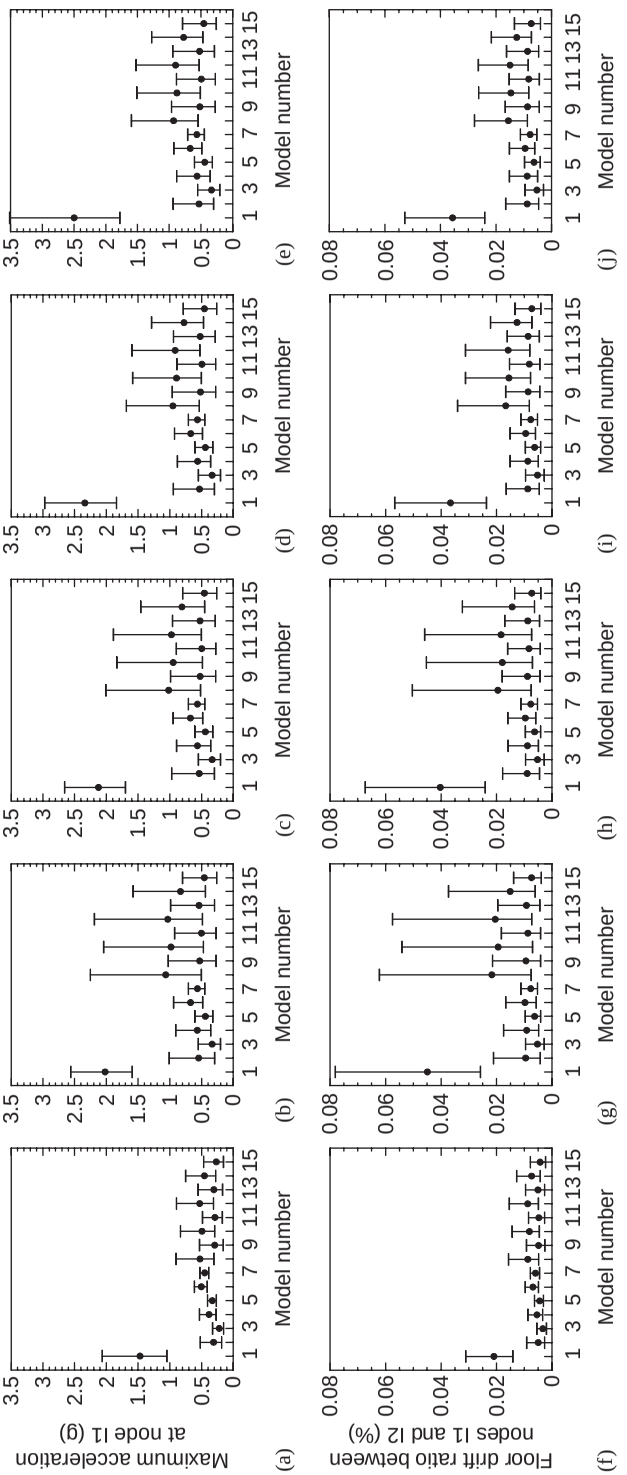

Figure 7. Sample acceleration and drift ratio demands for the Los Angeles earthquake histories. Acceleration: (a) Case I; (b) Case II; (c) Case III; (d) Case IV; (e) Case V and drift ratio: (f) Case I; (g) Case II; (h) Case III; (i) Case IV; (j) Case V.

DOI: 10.1002/eqe

Table III. Ratios of median responses in isolated and conventional NPPs.

Bearing type	Model number	Boston					Los Angeles				
		Case I	Case II	Case III	Case IV	Case V	Case I	Case II	Case III	Case IV	Case V
Acceleration at node I1											
FP	2	0.16	0.15	0.14	0.12	0.11	0.21	0.27	0.25	0.23	0.21
	3	0.16	0.15	0.14	0.12	0.11	0.15	0.17	0.16	0.14	0.13
	4	0.31	0.30	0.27	0.25	0.22	0.26	0.28	0.27	0.24	0.22
	5	0.31	0.30	0.27	0.25	0.22	0.22	0.22	0.21	0.19	0.18
	6	0.45	0.45	0.41	0.37	0.33	0.34	0.33	0.32	0.29	0.27
	7	0.45	0.44	0.41	0.36	0.33	0.31	0.28	0.27	0.24	0.23
LR	8	0.11	0.12	0.11	0.10	0.09	0.36	0.53	0.48	0.41	0.37
	9	0.07	0.08	0.07	0.06	0.06	0.20	0.26	0.25	0.22	0.21
	10	0.14	0.16	0.14	0.13	0.12	0.34	0.49	0.45	0.38	0.35
	11	0.10	0.11	0.10	0.09	0.08	0.20	0.25	0.23	0.21	0.20
LDR	12	0.06	0.08	0.07	0.07	0.06	0.36	0.51	0.46	0.39	0.36
	13	0.03	0.04	0.03	0.03	0.03	0.21	0.27	0.25	0.22	0.21
HDR	14	0.06	0.08	0.07	0.07	0.06	0.31	0.41	0.38	0.33	0.31
	15	0.03	0.04	0.04	0.04	0.03	0.18	0.23	0.21	0.19	0.18
	16	0.07	0.09	0.09	0.08	0.07	0.28	0.36	0.34	0.30	0.28
	17	0.04	0.06	0.05	0.05	0.04	0.17	0.21	0.20	0.19	0.17
Drift ratio between nodes I1 and I2											
FP	2	0.16	0.12	0.12	0.11	0.11	0.24	0.21	0.22	0.24	0.25
	3	0.15	0.12	0.11	0.11	0.11	0.16	0.12	0.13	0.14	0.15
	4	0.30	0.23	0.23	0.22	0.22	0.26	0.20	0.22	0.24	0.25
	5	0.30	0.23	0.23	0.22	0.22	0.21	0.14	0.16	0.17	0.18
	6	0.44	0.35	0.34	0.33	0.32	0.33	0.22	0.24	0.26	0.27
	7	0.44	0.34	0.33	0.33	0.32	0.28	0.17	0.19	0.21	0.22
LR	8	0.12	0.11	0.11	0.11	0.10	0.42	0.48	0.48	0.46	0.44
	9	0.09	0.07	0.07	0.07	0.07	0.23	0.21	0.22	0.24	0.24
	10	0.17	0.14	0.14	0.14	0.13	0.39	0.43	0.45	0.43	0.41
	11	0.13	0.10	0.10	0.10	0.09	0.23	0.19	0.21	0.22	0.23
LDR	12	0.07	0.08	0.08	0.07	0.07	0.42	0.46	0.46	0.43	0.42
	13	0.03	0.03	0.03	0.03	0.03	0.24	0.21	0.22	0.24	0.24
HDR	14	0.07	0.07	0.07	0.07	0.07	0.35	0.34	0.36	0.35	0.35
	15	0.04	0.04	0.04	0.04	0.04	0.20	0.16	0.18	0.20	0.21
	16	0.08	0.08	0.08	0.08	0.08	0.31	0.29	0.30	0.30	0.31
	17	0.04	0.05	0.05	0.05	0.04	0.19	0.15	0.17	0.18	0.19

the median response of the isolated NPP model divided by the median response of the conventional NPP model (Model 1).

Some general conclusions can be drawn on the basis of the data presented in Figures 6 and 7 and Table III. First, the use of seismic isolation leads to very significant reductions in acceleration

DOI: 10.1002/eqe

and drift demands. For a given type of isolation systems (e.g. LR bearings), the reductions in response are greater for the longer-period isolation system, which is an expected result, given the shapes of median spectra of Figure 4. Much greater percentage reductions are realized for the East Coast (Boston) histories because the West Coast (Los Angeles) histories have a much higher long-period content (see Figure 4(b) and (d)). Importantly, the spectral accelerations of some of the Los Angeles histories are greater at a period of 2 s than at 0.14 s: the first mode period of the internal structure.

For the Boston BDB shaking (Cases II–V), the increase in median and 84th percentile accelerations and drift ratios is significant for the conventional NPP but small for the isolated NPPs, showing that an increase in the shaking intensity does not produce a similar percentage increase in the demands on the secondary systems. The increase in yield strength of the internal structure increases the median value and dispersion of the acceleration responses in the conventional NPP but not in the isolated NPPs because, for the Boston earthquake histories, all of the isolated superstructures remained elastic for BDB earthquake shaking.

For the Los Angeles BDB histories and Case II yield strength (see Table II), the superstructures of the isolated models with a period of 2 s yield for 22 of the 40 earthquake histories. (The number of instances of yielding decreases with an increase in isolation period or superstructure strength.) Superstructure yielding for some of the earthquake histories produced the large differences in the 16th and 84th percentile responses of the 2-s isolated models in Figure 7. Nonetheless, the introduction of an isolation system reduces substantially the median response of the NPP building and its secondary systems.

Floor response spectra (FRS) have been widely used in the nuclear industry [25] to estimate demands on flexible secondary systems [16]. In this study, absolute acceleration response histories were recorded at node I2 of Figure 1(c) to develop representative FRS and to identify the difference in spectral responses for the conventional and isolated NPPs. (For the sample NPP under consideration, node I2 is located at the base of a tall steam generator.) Figure 8 shows the median and 84th percentile floor acceleration response spectra for models 1, 2, 9, 13, and 15 subjected to the Boston and Los Angeles SSE bins of ground motions, assuming that the peak responses are lognormally distributed. The frequency range of 5–33 Hz encompasses the frequencies of most NPP secondary systems. The reductions in FRS resulting from the use of seismic isolators range between 3 and 20+ for the selected isolation systems and the frequency range of 5–33 Hz. The largest reductions in response are realized for the East Coast (Boston) earthquake histories.

Figure 9 presents median, 16th and 84th percentile floor acceleration spectral values averaged over the frequency range from 5 to 33 Hz for each model, each case and each bin of histories. Table IV lists the ratios of the median responses of the isolated and conventional NPPs shown in Figure 9. The trends of Figure 9 are similar to those of Figures 6 and 7.

3.2. Comparison of secondary-system demands for different isolation systems

Section 3.1 showed that the use of seismic isolation can substantially reduce demands on secondary systems. A comparison of results by isolator type is presented here. For the lower intensity ground motions (i.e. Boston bin), the responses of the linear and lightly damped isolators (LDR) are smaller than those of the bilinear isolators (FP and LR), as seen in Tables III and IV. For the bilinear systems, seismic demands on the secondary systems increase as Q_d increases. For higher levels of earthquake shaking (i.e. Los Angeles bin), the secondary-system demands are comparable for bilinear and LDR systems with the same second-slope period. Table V presents the median

DOI: 10.1002/eqe

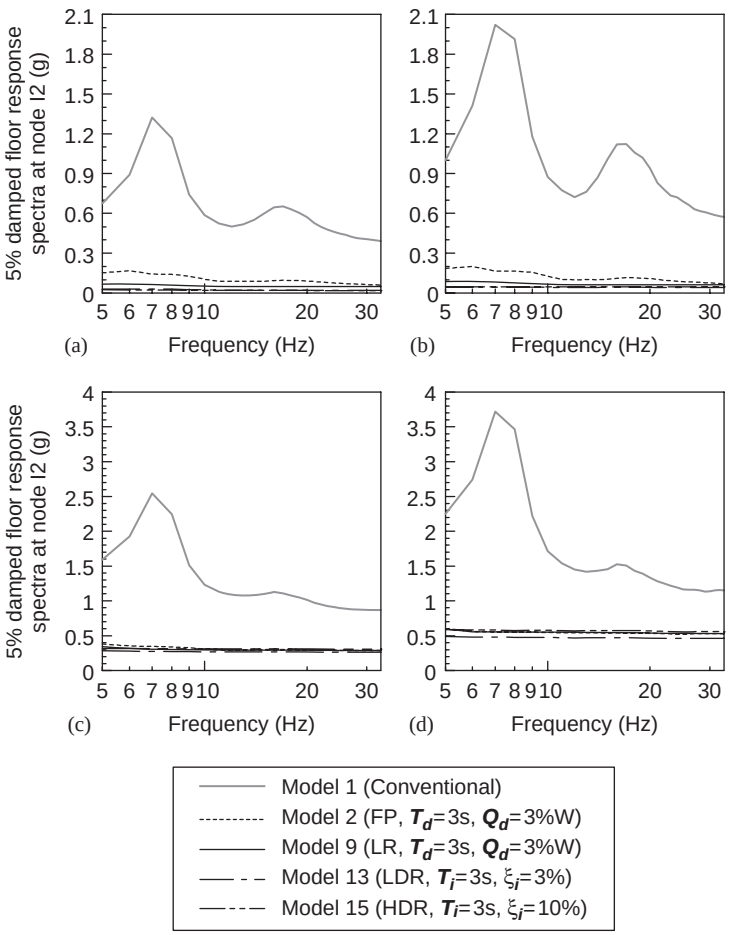

Figure 8. Median and 84th percentile floor response spectra at node I2 for Case 1. Boston: (a) Median and (b) 84th percentile. Los Angeles: (c) Median and (d) 84th percentile.

peak isolator displacements and the corresponding effective period[¶] for each isolated model, case, and earthquake bin. Isolator displacements are small for the Boston bin and the maximum shear force in the FP and LR systems is dominated by Q_d, which is the reason why the demands for the bilinear systems are higher than those for linear systems for which Q_d is zero if damping is ignored. The effective period better characterizes the seismic demands than the second-slope period. Consider Models 2 (FP) and 13 (LDR) that have the same second-slope (or elastic) isolation period of 3 s. For the Boston bin, the secondary-system demands for Model 2 are larger than those for Model 13 because the effective period for Model 2 is 50–70% of that for Model 13. The effect of Q_d is less significant for higher intensity shaking (Los Angeles bin) and these models because their effective periods are similar.

[¶] The effective period is based on K_{eff} shown in Figure 2.

DOI: 10.1002/eqe

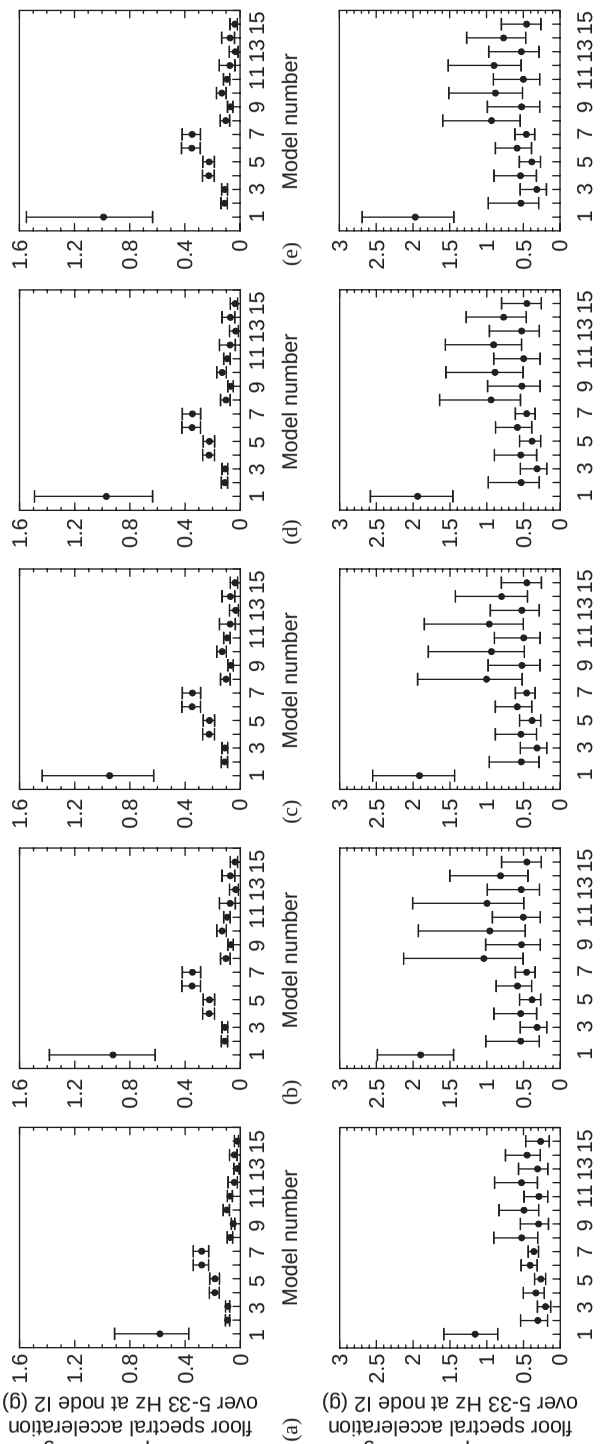

Figure 9. Average floor spectral accelerations at node I2. Boston: (a) Case I; (b) Case II; (c) Case III; (d) Case IV; and (e) Case V. Los Angeles: (f) Case I; (g) Case II; (h) Case III; (i) Case IV; and (j) Case V.

DOI: 10.1002/eqe

Table IV. Ratios of median FRS responses in isolated and conventional NPPs.

Bearing type	Model number	Boston					Los Angeles				
		Case I	Case II	Case III	Case IV	Case V	Case I	Case II	Case III	Case IV	Case V
FP	2	0.16	0.12	0.12	0.12	0.11	0.26	0.28	0.28	0.27	0.27
	3	0.15	0.12	0.12	0.11	0.11	0.17	0.17	0.16	0.16	0.16
	4	0.32	0.24	0.24	0.23	0.23	0.29	0.28	0.28	0.28	0.27
	5	0.31	0.24	0.24	0.23	0.23	0.23	0.20	0.20	0.20	0.19
	6	0.48	0.38	0.37	0.36	0.35	0.35	0.31	0.31	0.30	0.30
	7	0.48	0.38	0.37	0.36	0.35	0.31	0.24	0.24	0.24	0.23
LR	8	0.12	0.11	0.11	0.11	0.10	0.45	0.55	0.52	0.49	0.47
	9	0.09	0.07	0.07	0.07	0.07	0.26	0.28	0.27	0.27	0.27
	10	0.17	0.14	0.14	0.13	0.13	0.43	0.50	0.49	0.46	0.45
	11	0.13	0.10	0.10	0.10	0.09	0.25	0.27	0.26	0.26	0.25
LDR	12	0.07	0.08	0.08	0.08	0.07	0.46	0.52	0.50	0.47	0.46
	13	0.03	0.04	0.04	0.03	0.03	0.27	0.28	0.27	0.27	0.27
HDR	14	0.07	0.08	0.08	0.07	0.07	0.39	0.43	0.42	0.40	0.39
	15	0.04	0.04	0.04	0.04	0.04	0.23	0.24	0.24	0.23	0.23
	16	0.08	0.08	0.08	0.08	0.08	0.35	0.38	0.37	0.36	0.35
	17	0.05	0.05	0.05	0.05	0.05	0.22	0.23	0.22	0.22	0.22

The influence of viscous damping on secondary-system demands can be characterized by comparing the results for the LDR and HDR systems. Consider Models 13 (3% damping) and 15 (10% damping). The results of Tables III and IV show that the 3-fold increase in viscous damping has a minor (Boston bin) to moderate (Los Angeles bin) impact on secondary-system demands. An increase in isolator damping will reduce the isolator displacements and enable the construction of more compact elastomeric bearings.

3.3. Performance spaces

The performance space is an alternate method for comparing demands on secondary systems and explicitly accounting for uncertainty and randomness in demand and response prediction [26]. Herein, the performance space is defined by two response quantities (e.g. acceleration and drift) and an 84% probability that the responses will lie within the performance space. For example, Figure 10(a) presents the performance space associated with the drift ratio of node I1 and peak ground acceleration for the Boston SSE bin of earthquake histories. The choice of response quantities or indices used to define the performance space should be secondary-system dependent; typical quantities include maximum or spectral acceleration, velocity, and displacement. The position of performance space indicates the overall level of structural response, the area of the space captures the randomness and uncertainty, and the shape of the space identifies the relationship (e.g. linear dependence) between the two chosen indices.

The relationship between the two chosen indices of interest must first be defined to characterize the performance space. Herein, the joint probability density function (jpdf) of the two indices is

DOI: 10.1002/eqe

Table V. Median isolator displacements and effective periods for the isolation systems.

Bearing type	Model number	Boston					Los Angeles				
		Case I	Case II	Case III	Case IV	Case V	Case I	Case II	Case III	Case IV	Case V
Median isolator displacement (*m*)											
FP	2	0.021	0.046	0.046	0.046	0.046	0.543	1.037	1.037	1.037	1.037
	3	0.022	0.047	0.047	0.047	0.047	0.524	1.004	1.004	1.004	1.004
	4	0.013	0.031	0.031	0.031	0.031	0.422	0.878	0.878	0.878	0.878
	5	0.014	0.032	0.032	0.032	0.032	0.430	0.852	0.852	0.852	0.852
	6	0.010	0.023	0.023	0.023	0.023	0.335	0.754	0.759	0.754	0.754
	7	0.011	0.024	0.024	0.024	0.024	0.348	0.759	0.759	0.759	0.759
LR	8	0.024	0.046	0.046	0.046	0.046	0.474	0.875	0.875	0.876	0.876
	9	0.031	0.056	0.056	0.056	0.056	0.554	1.048	1.048	1.048	1.048
	10	0.020	0.039	0.039	0.039	0.039	0.397	0.779	0.779	0.780	0.780
	11	0.028	0.052	0.052	0.052	0.052	0.454	0.906	0.906	0.906	0.906
LDR	12	0.039	0.067	0.067	0.067	0.067	0.513	0.871	0.872	0.872	0.873
	13	0.038	0.065	0.065	0.065	0.065	0.667	1.133	1.133	1.134	1.134
HDR	14	0.032	0.055	0.055	0.055	0.055	0.416	0.706	0.706	0.706	0.706
	15	0.033	0.057	0.057	0.057	0.057	0.542	0.921	0.921	0.921	0.921
	16	0.027	0.047	0.047	0.047	0.047	0.334	0.567	0.567	0.567	0.567
	17	0.029	0.049	0.049	0.049	0.049	0.435	0.740	0.740	0.740	0.740
Effective period (*s*)											
FP	2	1.49	1.92	1.92	1.92	1.92	2.83	2.91	2.91	2.91	2.91
	3	1.59	2.14	2.14	2.14	2.14	3.61	3.78	3.78	3.78	3.78
	4	0.91	1.31	1.31	1.31	1.31	2.62	2.80	2.80	2.80	2.80
	5	0.94	1.39	1.39	1.39	1.39	3.21	3.54	3.54	3.54	3.54
	6	0.65	0.96	0.96	0.96	0.96	2.37	2.67	2.67	2.67	2.67
	7	0.71	1.00	1.00	1.00	1.00	2.81	3.30	3.30	3.30	3.30
LR	8	1.33	1.56	1.56	1.56	1.56	1.94	1.97	1.97	1.97	1.97
	9	1.69	2.03	2.03	2.03	2.03	2.83	2.91	2.91	2.91	2.91
	10	1.01	1.26	1.26	1.26	1.26	1.86	1.93	1.93	1.93	1.93
	11	1.25	1.58	1.58	1.58	1.58	2.64	2.80	2.80	2.80	2.80
LDR	12	2	2	2	2	2	2	2	2	2	2
	13	3	3	3	3	3	3	3	3	3	3
HDR	14	2	2	2	2	2	2	2	2	2	2
	15	3	3	3	3	3	3	3	3	3	3
	16	2	2	2	2	2	2	2	2	2	2
	17	3	3	3	3	3	3	3	3	3	3

assumed to be jointly lognormal. Figure 10 illustrates the calculation procedure. Figure 10(a) plots all 40 response points from the response-history analysis of the conventional NPP subjected to Case I and Boston ground motions. The peak ground acceleration and peak drift ratio at node I1

DOI: 10.1002/eqe

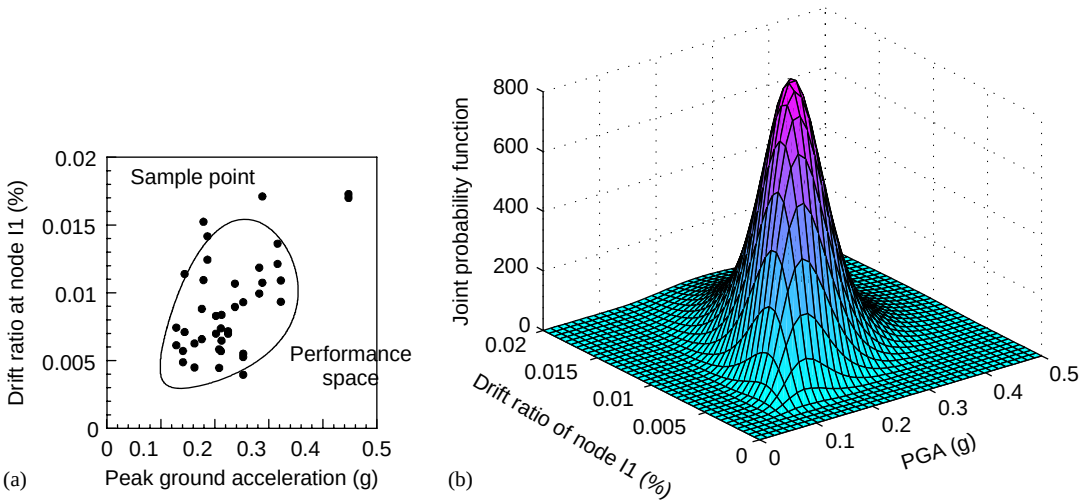

Figure 10. Performance space data for the Boston SSE bin of earthquake histories: (a) performance space and all sample points and (b) joint probability density function.

are denoted as two random variables, X and Y, respectively. The jpdf of X and Y is calculated by the following equation:

$$f_{XY} = \frac{1}{2\pi \cdot xy \cdot |\Sigma|^{0.5}} \exp[-0.5 \cdot (\tilde{z} - \tilde{m})^{\mathrm{T}} \Sigma^{-1} (\tilde{z} - \tilde{m})] \tag{3}$$

where $\tilde{z} = [\ln x \ \ln y]^{\mathrm{T}}$ and $\tilde{m}$ and Σ are the mean vector and covariance matrix of random variables $\ln X$ and $\ln Y$; $\tilde{m}$ and Σ can be estimated from the sample points shown in the figure. (Appendix A presents the derivation of Equation (3)). Figure 10(b) shows the jpdf for this case. The total volume under the surface of the function is 1; the area in the XY plane corresponding to 84% of the total volume is the performance space of Figure 10(a).

Figure 11 presents performance spaces defined by the 5% damped average floor spectrum acceleration at node I2 over a frequency range of 5–33 Hz and the drift ratio between nodes I1 and I2. This performance space captures force demands on acceleration-sensitive components and systems attached at node I2 and the deformation demands on displacement-sensitive components and systems attached at nodes I1 and I2. The performance spaces associated with the isolated NPP models are much closer to the origin and smaller in area than those of the conventional NPP (Model 1), indicating much smaller seismic demands of reduced variability on the secondary systems in the isolated NPPs. Median demands are reduced by a factor between 2 and 20. The performance spaces of Figure 12 permit a comparison of seismic demands on secondary systems for the conventional NPP and one isolated NPP (Model 11, lead–rubber isolators: see Table I) at the Boston and Los Angeles sites for the five cases of Table II. For the conventional NPP, the increase in demands (and absolute dispersion) on the secondary systems from SSE to BDB shaking is most significant compared with the changes in demand and dispersion for the isolated NPPs.

DOI: 10.1002/eqe

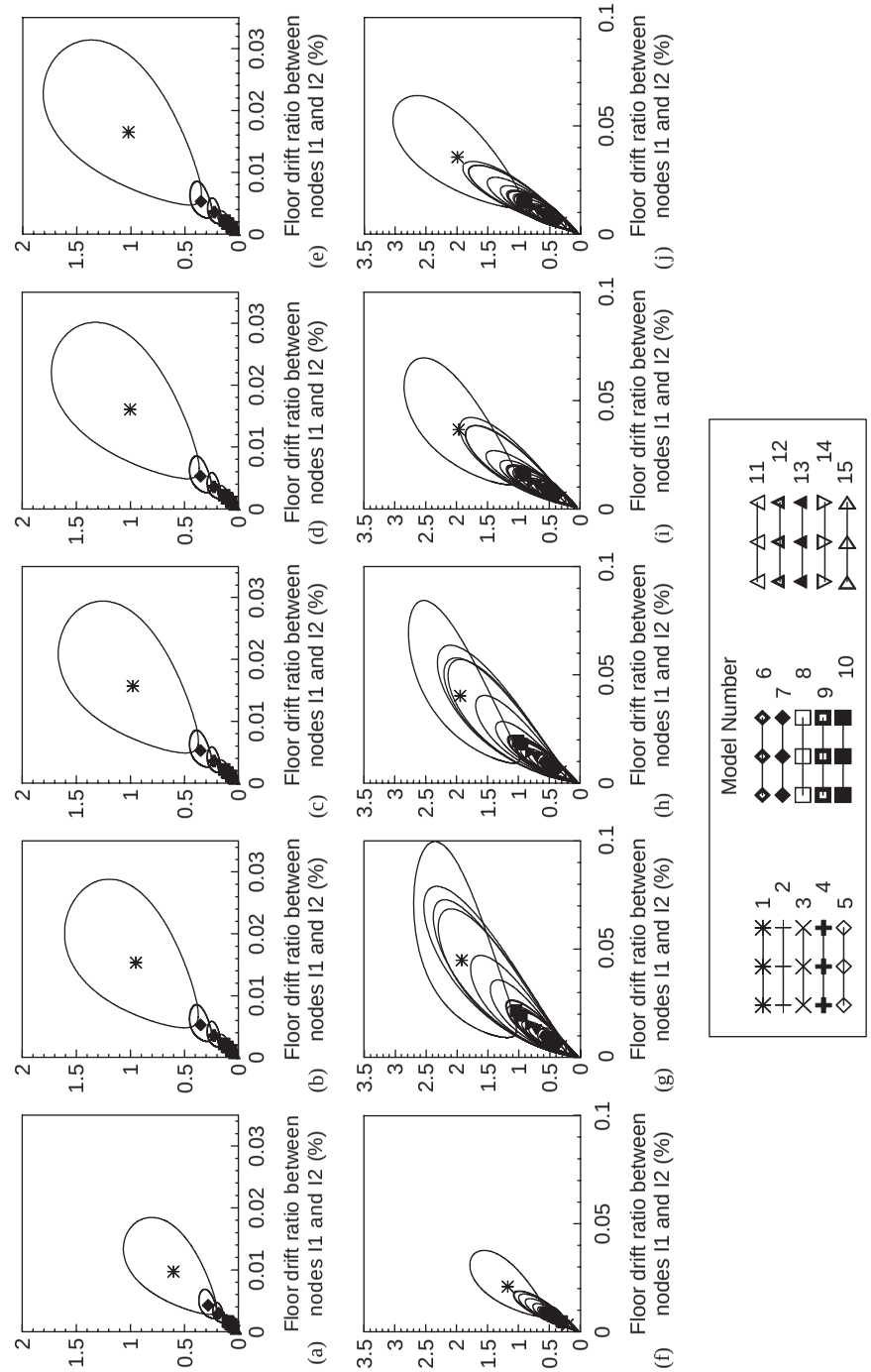

Figure 11. Performance spaces for all models and Cases I–V for Boston and Los Angeles. Boston: (a) Case I; (b) Case II; (c) Case III; (d) Case IV; and (e) Case V. Los Angeles: (f) Case I; (g) Case II; (h) Case III; (i) Case IV; and (j) Case V.

DOI: 10.1002/eqe

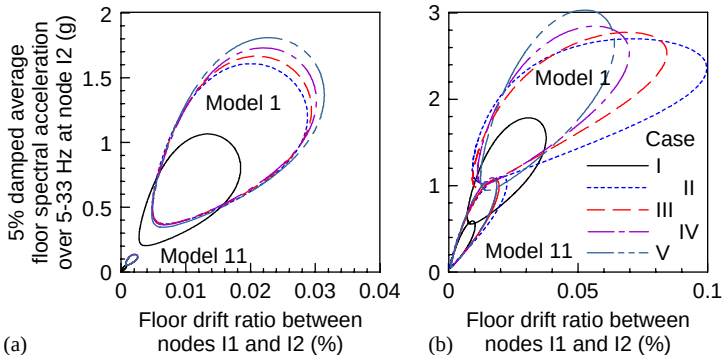

Figure 12. Performance spaces of Models 1 and 11 and Cases I–V: (a) models 1 and 11, Boston and (b) models 1 and 11, Los Angeles.

4. CLOSING REMARKS

Seventeen numerical models of a conventional and seismically isolated NPP reactor building of modern construction were studied to judge the effectiveness of protective systems to mitigate earthquake-induced demands on secondary systems. Response-history analysis of linear elastic and simple bilinear models of the reactor building was performed using earthquake histories associated with SSE and BDB earthquake shaking for East and West Coast sites in the United States. (Nonlinear action was permitted in the internal structure only; the containment structure was assumed to remain elastic for all levels of shaking.) Randomness in the seismic input at each site was considered by not spectrally matching the earthquake histories and only horizontal earthquake shaking was addressed. Approximate models of sliding and elastomeric bearings were employed for the analysis.

Seismic demands on secondary systems were presented for sample locations (points of attachment of a steam generator and piping) in the reactor building for each site, SSE and BDB shaking, and for linear and nonlinear response in the internal structure. For each suite of analyses, the introduction of protective systems, regardless of type, led to substantial reductions in the seismic demands on the sample secondary systems. Larger percentage reductions in demand were realized for the East Coast site (Boston bin) because the ratios of the ground-motion spectral ordinates at the fundamental period of the internal structure and the isolated periods of 2, 3, and 4 s were substantially larger for the East Coast motions. For lower levels of earthquake shaking (e.g. Boston bin), the characteristic strength of the bilinear FP and LR isolation systems has a major impact on the demands on the secondary systems. An increase in characteristic strength reduces the effective period, increases acceleration and drift demands in superstructures, and reduces median isolator displacements. For greater earthquake shaking (e.g. Los Angeles bin), the impact of characteristic strength is not as significant. The use of long-period isolators minimized the seismic demands on the secondary systems. However, other factors must be considered in the selection of isolator period and isolator type for NPP and SNF structures, including (a) the maximum permissible displacement across the isolation interface, (b) the feasibility of fabricating *long-period* elastomeric bearings, (c) operating-basis earthquake demands on the secondary systems, and (d) the effects of vertical earthquake shaking.

DOI: 10.1002/eqe

Performance spaces were introduced as one means of judging the seismic demands on secondary systems in NPP reactor buildings. The sample performance spaces clearly demonstrated the benefits of seismically isolating NPP and SNF buildings for both SSE and BDB shaking: median demands and absolute dispersions are reduced by factors ranging between 2 and 20.

APPENDIX A: DERIVATION OF THE JOINTLY LOGNORMAL DISTRIBUTION

Since the joint probability density function (jpdf) for X and Y is assumed to be jointly lognormal, the jpdf for $\ln X$ and $\ln Y$ should be jointly normal, namely,

$$f_{\ln X \ln Y} = \frac{1}{2\pi \cdot |\Sigma|^{0.5}} \exp[-0.5 \cdot (\tilde{z} - \tilde{m})^{\mathrm{T}} \Sigma^{-1} (\tilde{z} - \tilde{m})] \tag{A1}$$

where $\tilde{z}$, $\tilde{m}$, and Σ are as defined in Equation (3). The jpdf for X and Y is

$$f_{XY} = f_{\ln X \ln Y} \cdot |J| \tag{A2}$$

where J is the Jacobian of the transformation, equal to

$$J = \begin{bmatrix} \dfrac{\partial \ln x}{\partial x} & \dfrac{\partial \ln x}{\partial y} \\ \dfrac{\partial \ln y}{\partial x} & \dfrac{\partial \ln y}{\partial y} \end{bmatrix} = \frac{1}{xy} \tag{A3}$$

Equation (3) can thus be obtained by substituting Equation (A3) into Equation (A2).

ACKNOWLEDGEMENTS

Financial support for the studies described in this paper was provided in part by the Multidisciplinary Center for Earthquake Engineering Research (MCEER) through grants from the Earthquake Engineering Centers Program of the National Science Foundation (NSF), Award Number EEC-9701471, and the State of New York. The opinions, findings, conclusions expressed in this paper are those of the authors and do not necessarily reflect the views of the sponsors or the Research Foundation of the State University of New York. Dr Ayman Saudy and Mr Medhat Elgohary of Atomic Energy of Canada Limited (AECL) provided invaluable information on NPP reactor-building construction and secondary systems in the nuclear power plants and provided review comments on the paper. The MCEER/NSF and AECL support is gratefully acknowledged.

REFERENCES

1. U.S. Nuclear Regulatory Commission (USNRC). Identification and characterization of seismic sources and determination of safe shutdown earthquake ground motion. *Regulatory Guide 1.165*, U.S. Nuclear Regulatory Commission (USNRC), Washington, DC, 1997.
2. U.S. Nuclear Regulatory Commission (USNRC). *NRC Regulations—Title 10, Code of Federal Regulations*. U.S. Nuclear Regulatory Commission (USNRC), Washington, DC, 2005.
3. Kelly JM. Seismic isolation. *In Earthquake Engineering* (Chapter 11), Bozorgnia Y, Bertero VV (eds). CRC Press: Boca Raton, FL, 2004.
4. Buckle IG, Kelly TE, Jones LR. Basic concepts of seismic isolation and their application to nuclear structures. *Seismic Engineering Recent Advances in Design*, *Analysis*, *Testing and Qualification Methods* (ASME) 1987; **PVP-127**:429–437.

DOI: 10.1002/eqe

5. American Society of Civil Engineers (ASCE). Seismic analysis of safety-related nuclear structures and commentary. *ASCE 4-98*. American Society of Civil Engineers (ASCE), Reston, VA, 2000.
6. Malushte SR, Whittaker AS. Survey of past base isolation applications in nuclear power plants and challenges to industry/regulatory acceptance. *Proceedings of the 18th International Conference on Structural Mechanics in Reactor Technology*, Beijing, China. Atomic Energy Press: Beijing, 2005; 3404–3410.
7. Fan FG, Ahmadi G. Seismic responses of secondary systems in base-isolated structures. *Engineering Structures* 1992; **14**(1):35–48.
8. Kelly JM. The influence of base isolation on the seismic response of light secondary equipment. *Report No. UCB/EERC-81/17*, Earthquake Engineering Research Center, College of Engineering, University of California, Berkeley, CA, 1982.
9. Kelly JM, Tsai HC. Seismic response of light internal equipment in base isolated structures. *Report No. UCB/SESM-84/17*, Division of Structural Engineering and Structural Mechanics, Department of Civil Engineering, College of Engineering, University of California, Berkeley, CA, 1984.
10. Khechfe H, Noori M, Hou Z, Kelly JM, Ahmadi G. An experimental study on the seismic response of base-isolated secondary systems. *Journal of Pressure Vessel Technology* (ASME) 2002; **124**(1):81–88.
11. Takahashi K, Inoue K, Kato A, Morishita M, Fujita T. A development of three-dimensional seismic isolation for advanced reactor systems in Japan—Part 2. *Proceedings of the 18th International Conference on Structural Mechanics in Reactor Technology*, Beijing, China. Atomic Energy Press: Beijing, 2005; 3371–3380.
12. Suhara J, Matsumoto R, Oguri S, Okada Y, Inoue K, Takahashi K. Research on 3-D base isolation system applied to new power reactor 3-D seismic isolation device with rolling seal type air spring—Part 2. *Proceedings of the 18th International Conference on Structural Mechanics in Reactor Technology*, Beijing, China. Atomic Energy Press: Beijing, 2005; 3381–3391.
13. Shimada T, Suhara J, Takahashi K. Study on 3-dimensional base-isolation system applying to new type power plant reactor—Part 2 (hydraulic 3-dimensional base-isolation system). *Proceedings of the 18th International Conference on Structural Mechanics in Reactor Technology*, Beijing, China. Atomic Energy Press: Beijing, 2005; 3392–3403.
14. Okamura S, Kitamura S, Takahashi K, Somaki T. Experimental study on vertical component isolation system. *Proceedings of the 18th International Conference on Structural Mechanics in Reactor Technology*, Beijing, China. Atomic Energy Press: Beijing, 2005; 3411–3422.
15. Hadjian AH. On the decoupling of secondary systems for seismic analysis. *The Sixth World Conference on Earthquake Engineering*, New Delhi, India. Sarita Prakashan: Meerut, India, 1977; 3286–3291.
16. Chen Y, Soong TT. State-of-the-art review: seismic response of secondary systems. *Engineering Structures* 1988; **10**(4):218–228.
17. U.S. Nuclear Regulatory Commission (USNRC). *Standard Review Plan, Section 3.7.2, NUREG-0800*. U.S. Nuclear Regulatory Commission (USNRC), Washington, DC, 1996.
18. CSI. *SAP2000 User's Manual—Version 8.0*. Computers and Structures, Inc.: Berkeley, CA, 2002.
19. Mokha A, Constantinou MC, Reinhorn A. Teflon bearings in aseismic base isolation: experimental studies and mathematical modeling. *Technical Report NCEER-88-0038*, National Center for Earthquake Engineering Research, State University of New York, Buffalo, NY, 1988.
20. Constantinou MC, Tsopelas P, Kasalanati A, Wolff ED. Property modification factors for seismic isolation bearings. *Technical Report MCEER-99-0012*, Multidisciplinary Center for Earthquake Engineering Research, State University of New York, Buffalo, NY, 1999.
21. Fenz DM. Further development, testing and modeling of the Axon seismic isolation system. *Master Thesis*, Department of Civil, Structural and Environmental Engineering, State University of New York, Buffalo, NY, 2005.
22. Somerville P, Smith N, Punyamurthula S, Sun J. Development of ground motion time histories for phase 2 of the FEMA/SAC steel project. *Report SAC/BD-97/04*, SAC Joint Venture, Sacramento, CA, 1997.
23. Campbell KW. Development of semi-empirical attenuation relationships for CEUS. *Report to the U.S. Geological Survey*, Reston, VA, 2001.
24. Abrahamson NA, Silva WJ. Empirical response spectral attenuation relations for shallow crustal earthquakes. *Seismological Research Letters* 1997; **68**(1):94–127.
25. U.S. Nuclear Regulatory Commission (USNRC). Development of floor design response spectra for seismic design of floor-supported equipment or components. *Regulatory Guide 1.122*, U.S. Nuclear Regulatory Commission (USNRC), Washington, DC, 1978.
26. Astrella MJ, Whittaker AS. Changing the paradigm for performance-based seismic design. *International Workshop on Performance-Based Seismic Design—Concepts and Implementation*, Bled, Slovenia, 2004; 113–124.

DOI: 10.1002/eqe